THE JOURNAL OF BIOLOGICAL CHEMISTRY
Vol. 278, No. 10, Issue of March 7, pp. 8846–8852, 2003
Printed in U.S.A.

Overexpression of the Linker Histone-binding Protein tNASP Affects Progression through the Cell Cycle*

Received for publication, September 16, 2002, and in revised form, December 4, 2002
Published, JBC Papers in Press, December 30, 2002, DOI 10.1074/jbc.M210352200

Oleg M. Alekseev, David C. Bencic‡, Richard T. Richardson, Esther E. Widgren, and Michael G. O'Rand§

From the Department of Cell and Developmental Biology, University of North Carolina, Chapel Hill, North Carolina 27599-7090

NASP is an H1 histone-binding protein that is cell cycle-regulated and occurs in two major forms: tNASP, found in gametes, embryonic cells, and transformed cells; and sNASP, found in all rapidly dividing somatic cells (Richardson, R. T., Batova, I. N., Widgren, E. E., Zheng, L. X., Whitfield, M., Marzluff, W. F., and O'Rand, M. G. (2000) *J. Biol. Chem.* 275, 30378–30386). When full-length tNASP fused to green fluorescent protein (GFP) is transiently transfected into HeLa cells, it is efficiently transported into the nucleus within 2 h after translation in the cytoplasm, whereas the NASP nuclear localization signal (NLS) deletion mutant (NASP-ΔNLS-GFP) is retained in the cytoplasm. In HeLa cells synchronized by a double thymidine block and transiently transfected to overexpress full-length tNASP or NASP-ΔNLS, progression through the G_1/S border is delayed. Cells transiently transfected to overexpress the histone-binding site (HBS) deletion mutant (NASP-ΔHBS) or sNASP were not delayed in progression through the G_1/S border. By using a DNA supercoiling assay, *in vitro* binding data demonstrate that H1 histone-tNASP complexes can transfer H1 histones to DNA, whereas NASP-ΔHBS cannot. Measurement of NASP mobility in the nucleus by fluorescence recovery after photobleaching indicates that NASP mobility is virtually identical to that reported for H1 histones. These data suggest that NASP-H1 complexes exist in the nucleus and that tNASP can influence cell cycle progression through the G_1/S border through mediation of DNA-H1 histone binding.

Linker (H1) histones are involved in chromatin remodeling events and frequently exchange between numerous linker-binding sites on chromatin (2–4). Moreover, H1 histones have been shown to influence G_1/S phase progression (5) and in some cases inhibit transcription initiation (6). Consequently, understanding the role of H1 histones is important for our understanding of both gene activation and chromatin organization (7–9).

* This work was supported by NICHD, National Institutes of Health, through Cooperative Agreement U54HD35041 as part of the Specialized Cooperative Centers Program in Reproductive Research. The costs of publication of this article were defrayed in part by the payment of page charges. This article must therefore be hereby marked "*advertisement*" in accordance with 18 U.S.C. Section 1734 solely to indicate this fact.

‡ Present address: Integrated Toxicology Program, Nicholas School of the Environment, A333 LSRC, Science Dr., Duke University, Durham, NC 27708.

§ To whom correspondence should be addressed: Dept. of Cell and Developmental Biology, CB 7090, University of North Carolina, Chapel Hill, NC 27599-7090. Tel.: 919-966-5698; Fax: 919-966-1856; E-mail: morand@unc.edu.

H1 histones not bound to DNA appear to be bound to the H1 histone-binding protein NASP, which has been characterized previously *in vivo* and *in vitro* (1, 10, 11) as an acidic protein containing functional histone-binding sites, a leucine zipper, ATP/GTP-binding sites, and a functional nuclear localization signal (11, 12). NASP occurs in two major forms as follows: tNASP, found in gametes, embryonic cells, and transformed cells; and sNASP, found in all dividing somatic cells (1). Mouse sNASP (M_r 45,751) is identical to tNASP (M_r 83,934), except that it lacks two internal regions of the protein (1, 10). Similarly human tNASP and sNASP occur with identical deletions to those found in the mouse (10, 13).

During the cell cycle, *NASP* mRNA expression in somatic cells increases and decreases concurrently with histone mRNA changes in expression (1). However, in rapidly dividing cells protein levels of NASP remain fairly constant and only decrease to undetectable levels in non-dividing cells (1). Reports that overexpression of H1 histones can influence progression through the cell cycle (5) prompted us to investigate the effect on progression through the cell cycle by overexpression of *NASP* and to examine the relationship of NASP to H1 histones in HeLa cells. In this report we demonstrate that 1) the overexpression of *tNASP* does influence progression through the cycle, 2) tNASP is bound to H1 histones in HeLa cells, 3) *in vitro* complexes of tNASP-H1 will transfer H1 to DNA, and 4) that NASP and H1 have virtually identical mobilities within the nucleus.

EXPERIMENTAL PROCEDURES

All chemicals and reagents used in this study were molecular biology grade. Restriction enzymes were purchased from Roche Diagnostics. Purification of plasmid DNA and PCR products were carried out using QIAprep Miniprep and QIAquick PCR purification kits (Qiagen, Valencia, CA), and sequencing was performed at the University of North Carolina, Chapel Hill, automated sequencing facility. Affinity-purified goat anti-green fluorescent protein antiserum was purchased from Rockland (Gilbertsville, Pa); rabbit anti-histone H1 (FL-219) polyclonal antiserum was purchased from Santa Cruz Biotechnology (Santa Cruz, CA); and rabbit anti-NASP antiserum was prepared against either N-terminal (nucleotides 96–1099) or C-terminal (nucleotides 1100–2414) recombinant proteins as described previously (1).

Construction of Expression Vectors—The entire coding sequence of mouse tNASP (nucleotides 92–2405, GenBank™ accession number AF034610) was amplified from mouse testis Quick-clone cDNA (Clontech, Palo Alto, CA) using the Expand High Fidelity PCR System (Roche Molecular Biochemicals) and cloned into a *Kpn*I/*Bam*HI site in the pEGFP-N1 vector, which contains the sequence for expressing green fluorescent protein (GFP[1]; Clontech, Palo Alto, CA). The nuclear local-

[1] The abbreviations used are: GFP, green fluorescent protein; NLS, nuclear localization signal; HBS, histone-binding site; PBS, phosphate-buffered saline; FACS, fluorescent-activated cell sorting; HPLC, high pressure liquid chromatography; ACN, acetonitrile; FRAP, fluorescence recovery after photobleaching.

ization signal (NLS) deletion mutant (NASP-ΔNLS; nucleotides 92–2192), which lacked the nuclear localization signal (nucleotides 2215–2268), was PCR-amplified and cloned into the same pEGFP-N1 vector. The entire coding region of mouse sNASP (nucleotides 254–1384, GenBank™ accession number AF095722) (1) was also cloned into the pEGFP-N1 vector. The histone-binding site deletion mutant (NASP-ΔHBS; nucleotides 527–1384), which lacked all histone-binding sites (nucleotides 349–523) (11), was PCR-amplified and cloned into pEGFP-N1.

For cell cycle studies, vectors lacking the GFP sequence were constructed from pEGFP-N1 by excising the GFP by sequential digest by *Bam*HI and *Not*I. Digested ends were repaired by Klenow enzyme and ligated by T4 DNA ligase. All constructs were sequenced to verify the correct reading frame.

For *in vitro* H1-binding studies, full-length tNASP and NASP-ΔHBS (amino acids 567–773) were cloned into His_6 tag-pQE30 vectors. Recombinant proteins were expressed in BL21 (DE3) pLysS-competent *Escherichia coli* cells and purified on nickel-nitrilotriacetic acid-agarose columns (Qiagen, Valencia, CA).

Cell Studies—HeLa cells were maintained in Dulbecco's modified Eagle's medium-H plus 10% calf serum. Cells were removed from plastic dishes by trypsinization in EDTA. Synchronized populations of HeLa cells were obtained by double thymidine blocking as described previously (1).

Indirect Immunofluorescence—HeLa cells were grown on chamber slides with polystyrene wells (Falcon® CultureSlide, BD Biosciences), washed twice with cold (4 °C) PBS (phosphate-buffered saline, pH 7.0), fixed with chilled (−20 °C) methanol (20 min), washed twice with cold PBS, and incubated in rabbit anti-NASP (N-terminal) antiserum or preimmune serum (1:500) in PBS. Cells were incubated for 45 min, washed in PBS (3×, 5 min each), and incubated in fluorescein-conjugated, affinity-purified goat anti-rabbit IgG Fc fragment (1:1000 in PBS; Cappel, West Chester, PA) for 30 min. Washed cells were viewed with a Zeiss fluorescence microscope.

Chemical Transfection—Plasmid-DNA complexes were transiently transfected into HeLa cells using Effectene Transfection Reagent according to the manufacturer's instructions (Qiagen, Valencia, CA). This method is based on a non-liposomal lipid formulation and resulted in low cytotoxicity and high transfection efficiency (~97%) as determined by FACS analysis. Cells were transfected for 4–6 h with tNASP-GFP, NASP-ΔNLS-GFP, or GFP only. Transfection was confirmed by Western blotting. Lysates from HeLa cells transfected with tNASP-GFP or NASP-ΔNLS-GFP were separated by SDS-PAGE, Western-blotted (1), and stained with rabbit anti-NASP antibodies and affinity-purified goat anti-green fluorescent protein polyclonal antibodies (Rockland, Gilbertsville, PA).

Fluorescent-activated Cell Sorting (FACS) Analysis—Control cells and transfected cells 2, 4, 6, 8, and 24 h after release from the double thymidine block were washed with PBS, trypsinized, and fixed with 70% ethanol for ≥2 h on ice. Cells were washed in PBS, stained (30 min at 37 °C) with 50 μg/ml propidium iodide in PBS (containing 200 μg/ml RNase A and 0.1% Triton X-100), and incubated overnight at 4 °C before analysis at the University of North Carolina, Chapel Hill, Flow Cytometry Facility. For each sample at least 10,000 cells were counted. After gating out doublets and debris, cell cycle distribution was analyzed using Summit version 3.1 software (Cytomation, Inc., Fort Collins, CO). For each time point, at least three different samples were examined.

Immunoaffinity Chromatography—Affinity chromatography was carried out with rabbit anti-NASP (C-terminal) antibodies (30 mg) coupled to Reacti-Gel 6× beads (Pierce; coupling efficiency >80%). HeLa cells were trypsinized, washed twice with PBS, and solubilized by incubation in lysis buffer: 0.01 M sodium phosphate buffer, pH 7.2, 0.15 M NaCl, containing 1% Triton X-100, 0.5% sodium deoxycholate, and protease inhibitor mixture (Sigma) for 30 min on ice. Following centrifugation (10 min, 6000 × *g*), the pellet was sonicated, added to the supernatant, and centrifuged again (10 min, 6000 × *g*). The supernatant was collected and incubated with antibody-coupled beads overnight at 4 °C. After washing with PBS, the bound proteins were eluted from the beads with ImmunoPure® Elution Buffer (Pierce). The eluate pH was neutralized, and the sample was concentrated by vacuum centrifugation. Samples were separated by SDS-PAGE on 10–20% Tris-Cl Criterion gradient minigels (Bio-Rad) under reducing conditions, blotted to Immobilon-P (Millipore Inc., Bedford, MA), and probed for NASP and H1 histones. A C-18 reverse phase HPLC column (Waters, DeltaPak, 15 μM, 300 Å, 3.9 × 300 mm) equilibrated with acetonitrile (ACN) and 0.1% trifluoroacetic acid was used for the identification of histone H1 subtypes as described previously (1). Briefly, proteins were eluted at 28 °C with a multistep ACN in 0.1% trifluoroacetic acid gradient (0.7 ml/min). Gradients were developed from 18.5 to 100% buffer B (90% ACN in 0.1% trifluoroacetic acid) and 81.5 to 0% buffer A (10% ACN in 0.1% trifluoroacetic acid).

DNA Supercoiling Assay and H1-NASP Complexes—To assess the ability of H1-NASP complexes to transfer H1 to DNA, H1-NASP complexes were prepared *in vitro* and analyzed by a DNA supercoiling assay modified from the method of Kleinschmidt *et al.* (14). Calf thymus H1 histones (Roche Molecular Biochemicals) were biotinylated using an EZ-Link Sulfo-NHS-biotin kit (Pierce). Biotinylated H1 histones (1 μg) and tNASP (3 μg) were incubated (30 min at 37 °C in PBS containing 1 mM ATP) and chromatographed in 1× SSC buffer, pH 7.4, on Micro Bio-Spin 30 chromatography columns (Bio-Rad) to remove unbound H1 histones, which are retained by the column. Samples were evaluated by SDS-PAGE (10–20% Tris-HCl Criterion gels, Bio-Rad) and Western blotting to Immobilon-P membranes (Millipore, Bedford, MA). Biotinylated H1 histones were detected using alkaline phosphatase-conjugated avidin, and tNASP was detected using anti-NASP antibodies (N-terminal) and an alkaline phosphatase-conjugated secondary antibody (Cappel, West Chester, PA).

Supercoiled SV40 DNA (Invitrogen) was relaxed by incubation with topoisomerase I (Invitrogen). H1 histones, tNASP, or H1-NASP complexes from the Micro Bio-Spin 30 chromatography columns (described above) were incubated with the relaxed SV40 DNA for 30 min at 37 °C in TOPO buffer (50 mM Tris-HCl, 50 mM KCl, 10 mM $MgCl_2$, 0.1 mM EDTA, 0.5 mM dithiothreitol, 1.0 mM ATP, pH 7.5, with 30 μg/ml bovine serum albumin). The reactions were terminated by the addition of a Sarkosyl-proteinase K (2% and 0.3 mg/ml final concentration, respectively) mixture, which was incubated for 15 min at 37 °C. The DNA was subsequently phenol-chloroform-extracted, ethanol-precipitated, and analyzed by 1% agarose gel electrophoresis in 4× TAE and ethidium bromide-stained for visualization.

Fluorescence Recovery after Photobleaching (FRAP)—HeLa cells growing on coverslips (25–30% confluent) were transfected by pEGFPN1-NASP as described above. Cells were observed 24 h after transfection. Coverslips with cells were mounted in metal chambers and observed with a ×40 objective in a Zeiss 410 confocal microscope using the 488-nm laser line of an argon-krypton laser. In a FRAP experiment one scan of the unbleached cell was acquired, followed by a single bleach pulse of 5–10 s using a spot of rectangular shape and differing in size depending upon the size of the bleached structure (usually 50 or 100% of the nuclear area). Images were collected from the same section initially at 5- or 10-s intervals (1 min) followed by 30-s intervals for 4 min. For imaging, the laser power was attenuated to 0.3% of the bleach intensity. FRAP recovery curves were obtained from background-subtracted images using GelExpert Software (Nucleotech Corp., San Carlos, CA). The relative fluorescence in the nuclear area measured was determined as defined by Phair and Misteli (16). The relative fluorescence is $I_{rel} = T_0 I_t / T_t I_0$, where T_0 is the total nuclear fluorescence intensity before bleaching, and I_0 is the fluorescence intensity of the nuclear area to be bleached. T_t and I_t are the fluorescence intensities at time t. Approximately 1% of the fluorescence was lost during imaging.

RESULTS

Localization of NASP—Indirect immunofluorescent staining of unsynchronized HeLa cells as well as synchronized cells 2, 4, 6, and 8 h after being released from the double thymidine block demonstrated that immediately after mitosis and continuing throughout S and G_2 phases NASP is localized in both the nucleus and cytoplasm (Fig. 1*A*). In the nucleus NASP is unevenly distributed and appears to be excluded from nucleolar regions. In the cytoplasm NASP is most abundant in dense aggregations in the perinuclear regions but often can be seen as rows of aggregates reaching the peripheral cytoplasm (Fig. 1*A*).

Transfection of cells with tNASP-GFP resulted in strong nuclear staining (Fig. 1*B*) 2 h after transfection (97% of the cells were transfected after 24 h). Cytoplasmic staining remained weaker than the nuclear staining throughout the 24 h of observation. Transfection of cells with NASP-ΔNLS-GFP resulted in strong cytoplasmic staining, particularly in the perinuclear region, with no detectable stain in the nucleus (Fig. 1*C*). Control transfection with GFP only resulted in staining in both the nucleus and cytoplasm (Fig. 1*D*). Immunoprecipitation and Western blotting of transfected cells with anti-NASP

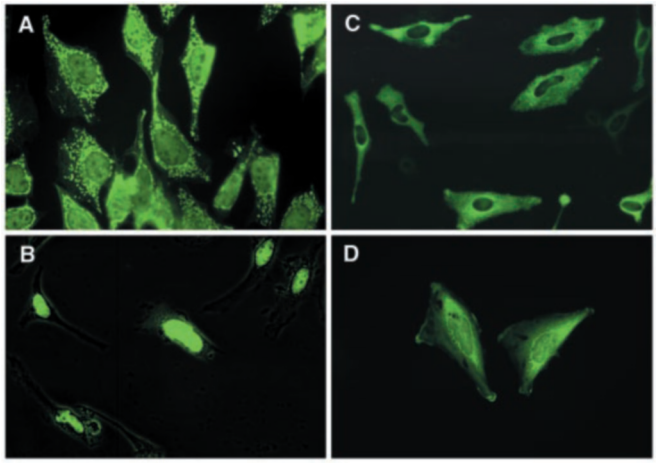

FIG. 1. **Localization of NASP in HeLa cells.** *A*, immunofluorescent localization of NASP in HeLa cells probed with rabbit anti-recombinant NASP. NASP appears in both the nucleus and cytoplasm. *B*, fluorescent localization of NASP in HeLa cells transfected with tNASP-GFP. *C*, fluorescent localization of NASP in HeLa cells transfected with the nuclear localization signal deletion mutant (NASP-ΔNLS-GFP). *D*, control. Fluorescent localization of GFP in HeLa cells transfected with GFP only. Original digital images were taken with a ×40 objective.

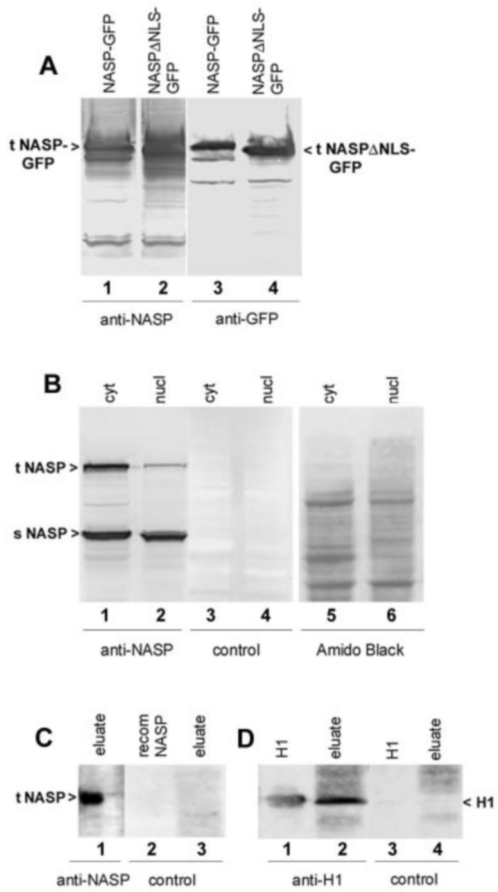

FIG. 2. **Western blot analysis of NASP in HeLa cells.** *A*, overexpression of tNASP-GFP (*lanes 1* and *3*) and NASP-ΔNLS-GFP (*lanes 2* and *4*) in HeLa cells. *Lanes 1* and *2* probed with rabbit anti-recombinant NASP. *Lanes 3* and *4* probed with anti-GFP. *B*, *lanes 1* and *2*, HeLa cell nuclear and cytoplasmic fractions probed with rabbit anti-recombinant NASP antibody. *Lanes 3* and *4*, HeLa cell nuclear and cytoplasmic fractions probed with rabbit preimmune serum. *Lanes 5* and *6*, Amido Black stain. Lanes were loaded with equal amounts of protein. *cyt*, cytoplasmic; *nucl*, nuclear fraction. *C*, *lane 1*, eluate from an anti-recombinant NASP antibody affinity column loaded with a HeLa cell lysate, probed with rabbit anti-recombinant NASP antibody. Control blots of recombinant NASP (*lane 2*) and affinity column eluate (*lane 3*) probed with anti-NASP antibody absorbed with recombinant NASP. *D*, *lane 1*, commercial H1 histones. *Lane 2*, eluate from an anti-recombinant NASP antibody affinity column loaded with a HeLa cell lysate, probed with rabbit anti-H1 histone antibody. Control blots of commercial H1 histones (*lane 3*) and affinity column eluate (*lane 4*) stained with goat anti-rabbit immunoglobulin (secondary antibody only).

and anti-GFP antiserum confirmed the expression of the constructs in these cells (Fig. 2*A*). Western blots of nuclear and cytoplasmic fractions from non-transfected HeLa cells confirmed the presence of both s and t forms of NASP in the nucleus and cytoplasm (Fig. 2*B*).

Association of H1 Histones with NASP—In myeloma 66-2 cells H1 histones were found to co-purify bound to native NASP (1). Similarly in HeLa cells, isolation of NASP by HPLC size chromatography or affinity chromatography with anti-NASP antibodies resulted in the co-purification of H1 histones (Fig. 2, *C* and *D*). Histone analysis by reverse phase HPLC of H1 histones extracted from H1-NASP complexes identified subtype $H1^{d/e}$ (H1.2) as the H1 histone (data not shown). Histone H1.2 is the most abundant subtype in HeLa cells (15); however, other histone H1 subtypes may not have been detected because of limited amounts of sample.

Effect of the Overexpression of NASP and NASP-ΔNLS on the Cell Cycle—In experiments overexpressing NASP and NASP deletion mutants in synchronized HeLa cells, we used constructs without the GFP sequence. Chemical transfection of cells with the vectors expressing NASP and NASP deletion mutants was done 24 h before the cells were released from the double thymidine block to ensure complete expression of the construct. Fig. 3 shows a typical experiment in which cell cycle progression is analyzed by FACS analysis up to 8 h after release from the double thymidine block. Overexpression of tNASP clearly affects the progression of cells through the cell cycle; compare Fig. 3, *A* and *B*. Similarly overexpression of NASP-ΔNLS affects the progression of cells through the cell cycle; compare Fig. 3, *A* and *C*. Fig. 3, *D* and *E*, shows that cells transfected with NASP-ΔHBS, the mutant lacking histone-binding sites, or sNASP do not delay progression through the cell cycle.

Table I presents the data collected from 6 independent experiments at 4 and 6 h after release from the double thymidine block. At 4 and 6 h after release there were significantly fewer HeLa cells, which were overexpressing tNASP, in the G_2 and S phases than there were non-overexpressing HeLa cells (71.45 *versus* 50.8%; $p = 0.01$ at 4 h, and 79.85 *versus* 60%; $p = 0.01$ at 6 h; Fig. 4 and Table I). Similarly there were significantly fewer overexpressing tNASP-ΔNLS HeLa cells than non-overexpressing cells in the G_2 and S phases (71.45 *versus* 53.17%; $p < 0.01$ at 4 h, and 79.85 *versus* 59.27%; $p = 0.01$ at 6 h; Fig. 4 and Table I). There was, however, no significant difference between tNASP and NASP-ΔNLS (Fig. 4). Data from 2, 8, and 24 h showed no significant differences between any of the cells tested. There was no difference in the progression of cells through the cell cycle between untreated cells and cells treated with delivery reagents only (Table I). At 4 and 6 h, cells transfected with NASP-ΔHBS ($p = 0.37$ (4 h) and $p = 0.48$ (6 h)) or sNASP ($p = 0.34$ (4 h) and $p = 0.34$ (6 h)) did not significantly delay progression through the cell cycle (Fig. 3, *D* and *E*; Table I). These data indicate that the overexpression of tNASP is different from the overexpression of sNASP in its effect on cell cycle progression and that the histone-binding sites are necessary for the delay in cell cycle progression. However, the presence of a NLS is not required for this effect.

DNA Supercoiling by H1-NASP Complexes—To test the ability of NASP to transfer H1 histones to DNA, calf thymus H1 histones were biotinylated and bound to tNASP *in vitro,* and the H1-NASP complexes were subsequently separated by chro-

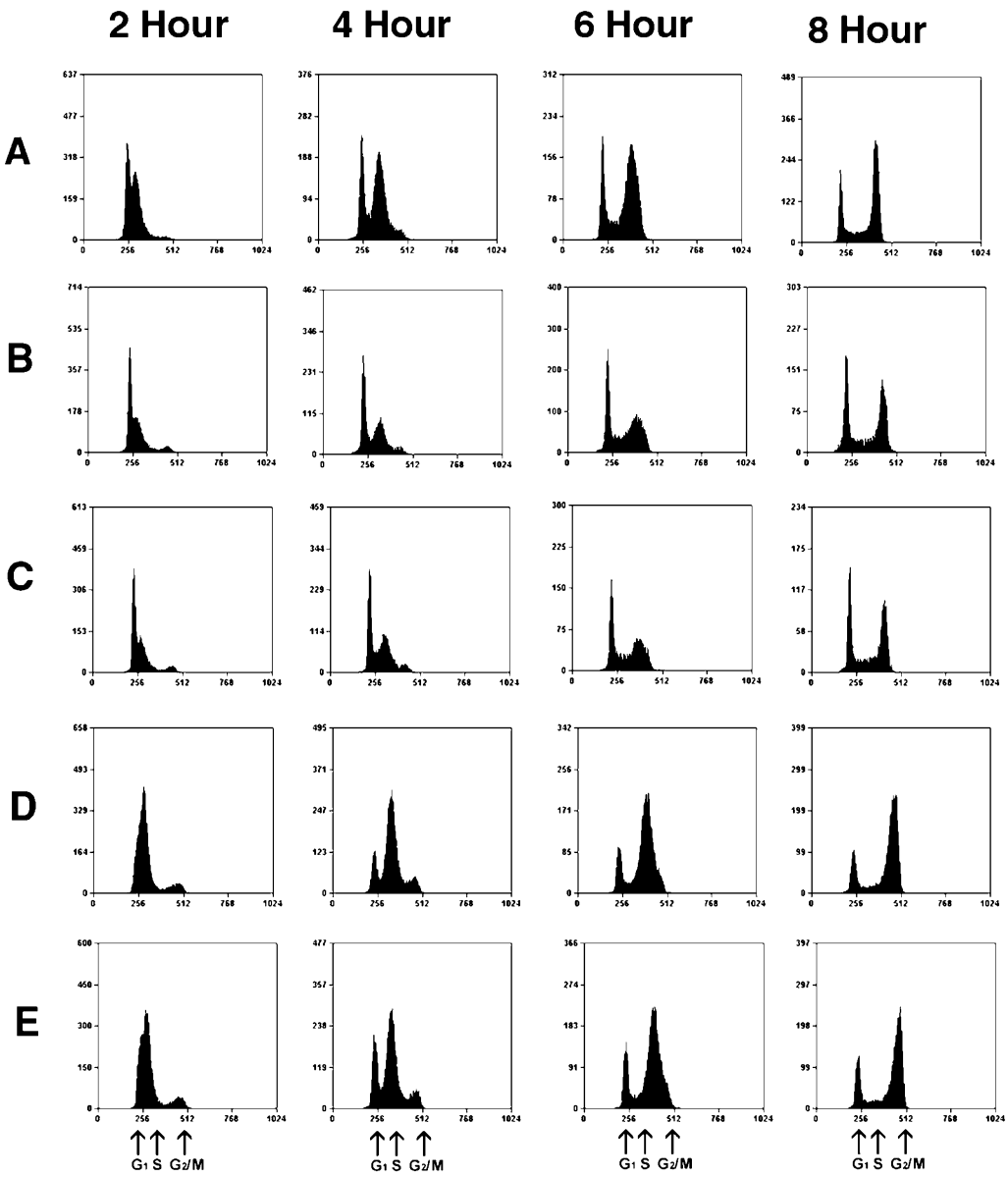

FIG. 3. **Cell cycle changes from overexpression of NASP in HeLa cells.** FACS analysis demonstrating double thymidine-blocked HeLa cells allowed to progress in synchrony through the cell cycle. *A*, normal progression through the cell cycle. *B*, overexpression of tNASP affects progression through the cell cycle. *C*, overexpression of NASP-ΔNLS (lacking nuclear localization signal) affects progression through the cell cycle. *D*, overexpression of NASP-ΔHBS (lacking histone binding sites) does not delay progression through the cell cycle. *E*, overexpression of sNASP (somatic NASP) does not delay progression through the cell cycle.

matography on Bio-Rad Micro Bio-Spin 30 (MBS30) columns. MBS30 columns separate H1-NASP complexes from unbound histones. Fig. 5 demonstrates that biotinylated H1 histones are retained on the MBS30 column (*lanes 1* and *2*); however, when H1 is complexed with NASP, both are eluted from the column (*lanes 4* and *6*). When NASP-ΔHBS is substituted for tNASP, it elutes from the column (*lane 5*) but does not bind H1 histones and does not non-specifically carry H1 histones through the column (*lane 3*).

The separated H1-NASP complexes were incubated with relaxed SV40 DNA to test the ability of H1 histones to supercoil the SV40 DNA (Fig. 6). Supercoiled and relaxed SV40 DNA are shown in Fig. 6, *lanes 1* and *2*. The addition of H1 histones to relaxed SV40 DNA causes supercoiling (*lane 3*), whereas the addition of tNASP does not (*lane 4*). As shown in Fig. 6, *lanes 6* and *7*, the addition of H1-NASP complexes, which have passed through the MBS30 column, to relaxed SV40 DNA results in supercoiling the DNA. If H1 only is chromatographed and the resulting eluate incubated with relaxed SV40 DNA, no supercoiling occurs because the H1 histones are retained by the column (*lane 5*). If increasing amounts of tNASP are added at the time of the addition of H1-NASP complexes to relaxed SV40 DNA, then there is a reduction in the intensity of the supercoiled DNA bands (Fig. 7). This indicates that tNASP competes with DNA for H1 binding.

Mobility of NASP in the Nucleus—Given our results that NASP and H1 histones co-purify from HeLa cells and that NASP can transfer H1 histones to DNA *in vitro*, it is possible that H1 histones not bound to DNA are bound to NASP. If NASP-H1 complexes were present in the nucleus, then we would expect that the mobility properties of NASP would be similar to those of H1. Consequently, we used FRAP to determine the time necessary for NASP to move into a bleached area of the nucleus. Bleaching ~50% of a nucleus containing tNASP-GFP (see also Fig. 1*B*) resulted in a recovery of fluorescence to a plateau level of 92.5 ± 4.6% in 220–225 s (n = 3 experi-

TABLE I
Percent of cells in S+G_2 phase

The abbreviations used are as follows: N, normal HeLa cells; tN, full-length tNASP sequence; NLS-, NASP-ΔNLS; HBS-, NASP-ΔHBS; sN, full-length sNASP; *t* test = Student's *t* test; NS, not significant.

4 h	Normal	tNASP full-length	NLS-mutant	HBS-mutant	sNASP full-length	Delivery reagent	*p* value
Exp. 1	60.70	42.90	49.30				
Exp. 2	62.90	52.20	52.80				
Exp. 3	71.30	57.30	57.40				
Exp. 4	86.70			88.10	73.60		
Exp. 5	70.10			53.10	46.40		
Exp. 6	77.00			86.90	79.40	79.30	
Mean	71.45	50.80	53.17	76.03	66.47		
S.D.	9.53	7.30	4.06	19.87	17.62		
t test, N *vs.* tN		0.01					$p = 0.01$
t test, N *vs.* NLS-			0.003				$p < 0.01$
t test, N *vs.* HBS-				0.37			NS
t test, N *vs.* sN					0.34		NS
6 h	**Normal**	**tNASP full-length**	**NLS-mutant**	**HBS-mutant**	**sNASP full-length**	**Delivery reagent**	***p* value**
Exp. 1	72.90	51.20	50.10				
Exp. 2	71.60	61.50	63.70				
Exp. 3	78.80	67.30	64.00				
Exp. 4	88.50			88.60	81.00		
Exp. 5	78.50			61.30	56.40		
Exp. 6	88.80			87.90	88.00	88.80	
Mean	79.85	60.00	59.27	79.27	75.13		
S.D.	7.41	8.15	7.94	15.56	16.60		
t test, N *vs.* tN		0.01					$p = 0.01$
t test, N *vs.* NLS-			0.01				$p = 0.01$
t test, N *vs.* HBS-				0.48			NS
t test, N *vs.* sN					0.34		NS

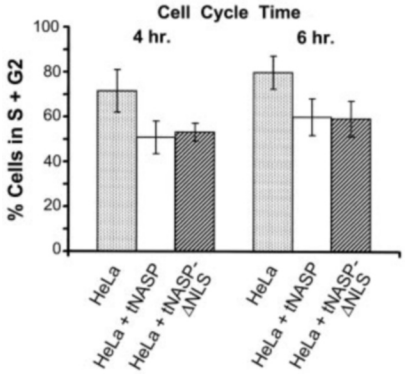

FIG. 4. **Comparison of cells in S + G_2 at 4 and 6 h after overexpression of tNASP or tNASP-ΔNLS in HeLa cells.** *Error bars* represent ± S.D. Cells overexpressing either tNASP or tNASP-ΔNLS are significantly different from the non-overexpressing HeLa cells but not from each other, see Table I.

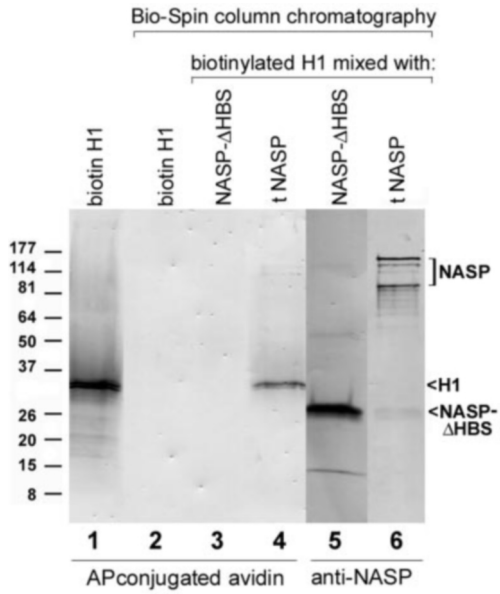

FIG. 5. **Western blot showing binding of H1 histones to tNASP but not NASP-ΔHBS.** *Lanes 1–4*, biotinylated H1 histones stained with alkaline phosphatase (*AP*)-conjugated avidin. *Lanes 5* and *6*, NASP stained with rabbit anti-recombinant NASP and an alkaline phosphatase-conjugated secondary antibody. *Lane 1*, control. Biotinylated H1 (1 μg) *not* chromatographed on a Micro Bio-Spin 30 column. *Lane 2*, negative. Biotinylated H1 (1 μg) chromatographed on and retained by a Micro Bio-Spin 30 column. *Lane 3*, negative. Biotinylated H1 (1 μg) + NASP-ΔHBS (3 μg) chromatographed on a Micro Bio-Spin 30 column with the biotinylated H1 retained. *Lane 4*, biotinylated H1 (1 μg) + tNASP (3 μg) chromatographed on a Micro Bio-Spin 30 column with the biotinylated H1 carried by the tNASP. *Lane 5*, biotinylated H1 (1 μg) + NASP-ΔHBS (3 μg) chromatographed on a Micro Bio-Spin 30 column with biotinylated H1 not bound by the NASP-ΔHBS, anti-NASP probed. *Lane 6*, biotinylated H1 (1 μg) + tNASP (3 μg) chromatographed on a Micro Bio-Spin 30 column with the biotinylated H1 carried by the tNASP, anti-NASP probed.

ments). Fig. 8 shows a typical experiment in which 50% of the nucleus was bleached (Fig. 8*A*), and the fluorescence recovery was 96.5 ± 1.2% in 225 s (Fig. 8*B*). This compares favorably to the 200–250 s necessary for recovery of H1-GFP fluorescence in the nucleus (4). As fluorescence intensity increases in the bleached area, there is a concomitant decrease in intensity in the unbleached area (Fig. 8*A*), indicating that NASP is redistributed within the nucleus. Because HeLa cells transfected with tNASP-GFP have very little tNASP-GFP in the cytoplasm (Fig. 1*B*), photobleaching the entire nucleus resulted in no recovery of fluorescence in 300 s ($n = 3$ experiments), indicating that essentially no tNASP-GFP entered the nucleus from the cytoplasm in these experiments.

DISCUSSION

In this study we have demonstrated that the H1 histone-binding protein NASP is present in the nucleus and cytoplasm of HeLa cells and can be directed to the nucleus by its NLS

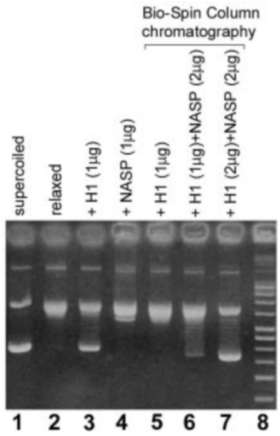

FIG. 6. **Transfer of H1 histones to DNA from tNASP using a DNA-supercoiling assay.** *Lane 1*, supercoiled SV40 DNA. *Lane 2*, relaxed SV40 DNA, supercoiled SV40 DNA relaxed with topoisomerase I. *Lane 3*, relaxed SV40 DNA with increased supercoiling due to addition of H1 (1 μg). *Lane 4*, relaxed SV40 DNA with no supercoiling induced by added tNASP (1 μg). *Lanes 5–7*, samples chromatographed on a Micro Bio-Spin 30 column (see Fig. 5). *Lane 5*, H1 (1 μg), control H1 was retained by the column and consequently no supercoiling was detected. *Lane 6*, H1 (1 μg) + tNASP (2 μg). *Lane 7*, H1 (2 μg) + tNASP (2 μg). In the presence of tNASP, the H1-tNASP complex forms, passes through the column, and subsequently increases DNA supercoiling. *Lane 8*, supercoiled DNA standard sizes: 16,210, 14,174, 12,138, 10,102, 8,066, 7,045, 6,030, 5,012, 3,990, 2,972, and 2,067 bp.

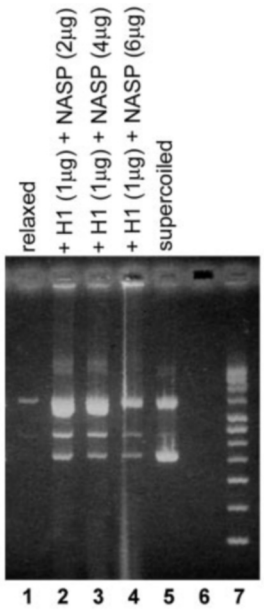

FIG. 7. **Competition of DNA and tNASP for H1.** *Lane 1*, relaxed SV40 DNA, supercoiled SV40 DNA relaxed with topoisomerase I. *Lane 2*, H1 (1 μg) + tNASP (2 μg), supercoiling of relaxed SV40 DNA due to transfer of H1 from NASP. *Lane 3*, H1 (1 μg) + tNASP (2 μg) + additional tNASP (2 μg); in the presence of additional (2 μg) tNASP, competition between tNASP and DNA for H1-reduced DNA supercoiling. *Lane 4*, H1 (1 μg) + tNASP (2 μg) + additional tNASP (4 μg); in the presence of additional (4 μg) tNASP, competition between tNASP and DNA for H1 reduced DNA supercoiling further. *Lane 5*, control supercoiled SV40 DNA. *Lane 6*, blank. *Lane 7*, supercoiled DNA standard sizes: 16,210, 14,174, 12,138, 10,102, 8,066, 7,045, 6,030, 5,012, 3,990, 2,972, and 2,067 bp.

(Fig. 1). Even though transfection of cells with tNASP-GFP resulted in almost complete nuclear localization of the construct, endogenous NASP is clearly not exclusively in the nucleus (Figs. 1 and 2). From Western blotting (Fig. 2) it would appear that there is less tNASP in the nucleus than in the cytoplasm, whereas sNASP is more evenly distributed between

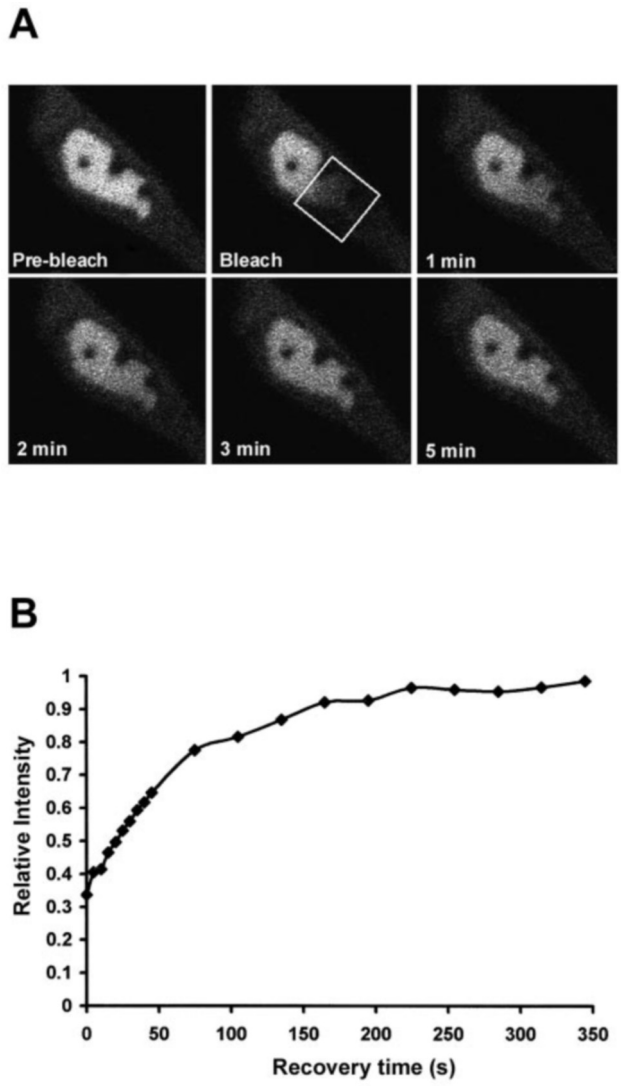

FIG. 8. **FRAP of tNASP in HeLa cell nucleus.** *A*, bleach and recovery of fluorescent GFP-tNASP in a HeLa cell nucleus. The HeLa cell was transfected with GFP-tNASP. The *rectangle* in the *bleach panel* indicates the size of the bleached area. *B*, relative recovery of fluorescence intensity in the nucleus shown in *A*; 96.5% recovery in 225 s.

the two compartments. Because tNASP occurs in rapidly dividing cell populations (gametes, embryonic cells, and transformed cells), its presence in the cytoplasm may serve as a storage site for excess linker (H1) histones. Alternatively, the majority of NASP in the cytoplasm could simply reflect a lagging degradation mechanism in rapidly dividing cells because in normal somatic cells there is little or no NASP in the cytoplasm (1).

Overexpression of tNASP significantly delays the progression of cells through the cell cycle, and surprisingly, overexpression of NASP-ΔNLS also significantly delays progression through the cell cycle (Fig. 3 and Table I). However, overexpression of sNASP does not appear to have a significant effect. The most obvious difference between tNASP (M_r 83,934) and sNASP (M_r 45,751) is the presence of an additional histone-binding site (1, 11). The identical C-terminal sequences of tNASP and sNASP contain a leucine zipper flanked by coiled coil regions downstream and possible DNA-binding sites upstream; these structural features are often indicative of protein dimers that bind DNA (17). If tNASP dimers form in the cytoplasm and bind H1 histones, then the overexpression of tNASP may result in insufficient linker histones for DNA rep-

lication. The only other notable difference between tNASP and sNASP is the presence of two additional ATP/GTP-binding sites in tNASP. These sites may be important for the functional attributes of tNASP and its role in chromatin remodeling.

Additionally, this study has demonstrated *in vitro* that H1-NASP complexes can cause the supercoiling of relaxed SV40 DNA by transferring H1 from NASP to DNA and importantly that excess tNASP can compete with DNA for H1. Kleinschmidt *et al.* (14) first demonstrated the transfer of histone to DNA from the *Xenopus laevis* form of NASP (N1/N2). Consequently, our results are consistent with the hypothesis that an equilibrium exists between NASP-H1 histone complexes and H1 histones bound to DNA. This equilibrium influences the availability of H1 histones to DNA and affects the progression of the cell through the G_1/S phase transition. It can be upset by overexpression of tNASP with its extra histone-binding site and is consistent with the observation that H1 histone overexpression has been shown to slow G_1/S phase progression (5) and in some cases inhibit transcription initiation (6).

Recent reports of the mobility of H1 histones in the nucleus (3, 4) concluded that an intermediate (4) or modulating protein (3) might be present to regulate the movement of H1. By using FRAP experiments on HeLa cells, this study has demonstrated that the mobility of NASP in the nucleus is essentially the same as that of H1 histones (Fig. 8). Although it could be fortuitous that the recovery times are similar, one interpretation of this result is that NASP and H1 have identical mobility characteristics because they are in a complex together in the nucleus. This interpretation is supported by the results from the co-precipitation experiments (Fig. 2). The recovery times of NASP and H1 (~225 s) differ markedly from other nuclear proteins. For example, GFP-HMG-17 and GFP-SF2/ASF have recovery times on the order of 30 s, whereas histone H2B has no recovery over 90 s (16). The less mobile (immobile) fraction determined in a FRAP experiment is a reflection of the residence time of the molecule in a compartment or complex and can be modified by various treatments such as acetylation (4). Small immobile fractions (~10%, *e.g.* GFP-SF2/ASF (16)) indicate that most of the molecules are replaced within the measured time, while large immobile fractions indicate that very few of the molecules are replaced. Histone H2B would appear to be replaced in the nucleosome very infrequently (16), whereas H1 histones are replaced every 200–250 s (4). The immobile fractions of NASP and H1 vary (~3.5% NASP *versus* ~9–26% for H1), but their recovery times (~225 s) are similar, which may indicate populations of H1 and NASP that are not complexed with each other or are in different phosphorylation or acetylation states. Phosphorylation of linker histones is known to inhibit chromatin remodeling (2, 18), and NASP may serve to mediate such interactions. Taken together, the results presented in this study indicate that NASP is most likely the H1-regulating protein in the nucleus and that a dynamic equilibrium exists between NASP-H1 complexes and DNA.

Acknowledgments—We thank Drs. J. Gordon and B. Muller-Borer for help and expertise with the FRAP experiments.

REFERENCES

1. Richardson, R. T., Batova, I. N., Widgren, E. E., Zheng, L. X., Whitfield, M., Marzluff, W. F., and O'Rand, M. G. (2000) *J. Biol. Chem.* **275,** 30378–30386
2. Horn, P. J., Carruthers, L. M., Logie, C., Hill, D. A., Solomon, M. J., Wade, P. A., Imbalzano, A. N., Hansen, J. C., and Peterson, C. L. (2002) *Nat. Struct. Biol.* **9,** 263–267
3. Lever, M. A., Th'ng, J. P. H., Sun, X. J., and Hendzel, M. J. (2000) *Nature* **408,** 873–876
4. Misteli, T., Gunjan, A., Hock, R., Bustin, M., and Brown, D. T. (2000) *Nature* **408,** 877–881
5. Brown, D. T., Alexander, B. T., and Sittman, D. B. (1996) *Nucleic Acids Res.* **24,** 486–493
6. Cheung, E., Zarifyan, A. S., and Kraus, W. L. (2002) *Mol. Cell. Biol.* **22,** 2463–2471
7. Karetsou, Z., Sandaltzopoulos, R., Frangou-Lazaridis, M., Lai, C.-Y., Tsolas, O., Becker, P. B., and Papamarcaki, T. (1998) *Nucleic Acids Res.* **26,** 3111–3118
8. Nagpal, S., Ghosn, C., DiSepio, D., Molina, Y., Sutter, M., Klein, E. S., and Chandraratna, R. A. S. (1999) *J. Biol. Chem.* **274,** 22563–22568
9. Gunjan, A., Sittman, D. B., and Brown, D. T. (2001) *J. Biol. Chem.* **276,** 3635–3640
10. Richardson, R. T., Bencic, D. C., and O'Rand, M. G. (2001) *Gene* (*Amst.*) **274,** 67–75
11. O'Rand, M. G., Batova, I., and Richardson, R. T. (2000) in *The Testis, From Stem Cell to Sperm Function* (Goldberg, E., ed) pp. 43–150, Springer-Verlag Inc., New York
12. Batova, I., and O'Rand, M. G. (1996) *Biol. Reprod.* **54,** 1238–1244
13. O'Rand, M. G., Richardson, R. T., Zimmerman, L. J., and Widgren, E. E. (1992) *Dev. Biol.* **154,** 37–44
14. Kleinschmidt, J. A., Fortkamp, E., Krohne, G., Zentgraf, H., and Franke, W. W. (1985) *J. Biol. Chem.* **260,** 1166–1176
15. Kratzmeier, M., Albig, W., Meergans, T., and Doenecke, D. (1999) *Biochem. J.* **337,** 319–327
16. Phair, R., and Misteli, T. (2000) *Nature* **404,** 604–609
17. Vinson, C. R., Sigler, P. B., and McKnight, S. L. (1989) *Science* **246,** 911–916
18. Peterson, C. L. (2002) *EMBO Rep.* **3,** 319–322